

Interactions of fatty acids with phosphatidylethanolamine membranes: X-ray diffraction and molecular dynamics studies

Arnaud Cordoní,^{1,*} Jesús Prades,^{1,†} Juan Frau,[§] Oliver Vögler,[†] Sérgio S. Funari,^{**} Juan J. Perez,^{*} Pablo V. Escribá,[†] and Francisca Barceló^{2,†}

Department d'Enginyeria Química,* Technical University of Catalonia, Barcelona, Spain; Laboratory of Molecular and Cellular Biomedicine[†] and Department of Chemistry,[§] University of the Balearic Islands, Palma de Mallorca, Spain; and HASYLAB,^{**} Hamburg, Germany

Abstract An experimental and theoretical study on 1,2-diacyl-*sn*-glycero-3-phosphoethanolamine (DEPE) membranes containing fatty acids (FAs) was performed by means of X-ray diffraction analysis and molecular dynamics (MD) simulations. The study was aimed at understanding the interactions of several structurally related FAs with biomembranes, which is necessary for further rational lipid drug design in membrane-lipid therapy. The main effect of FAs was to promote the formation of a H_{II} phase, despite a stabilization of the coexisting L_α + H_{II} phases. Derivatives of OA exhibited a specific density profile in the direction perpendicular to the bilayer that reflects differences in the relative localization of the carboxylate group within the polar region of the membrane as well as in the degree of membrane penetration of the FA acyl chain. Hydroxyl and methyl substituents at carbon-2 in the FA acyl chain were identified as effective modulators of the position of carboxylate group in the lipid bilayer. Our data highlight the specific potential of each FA in modulating the membrane structure properties.—Cordoní, A., J. Prades, J. Frau, O. Vögler, S. S. Funari, J. J. Perez, P. V. Escribá, and F. Barceló. **Interactions of fatty acids with phosphatidylethanolamine membranes: X-ray diffraction and molecular dynamics studies.** *J. Lipid Res.* 2010. 51: 1113–1124.

Supplementary key words fatty acid • molecular dynamics simulation • phosphoethanolamine membrane

It is a well-known fact that dietary fat uptake influences the fatty acid (FA) composition of cellular membranes. For example, the Mediterranean diet characterized by a high consumption of olive oil, which contains a large proportion of oleic acid (~80%), was associated with increases in the levels of this FA in various plasma membrane lipid species in rat and human cells (1, 2). Such a change in FA composition has a substantial impact on structural membrane properties. Indeed, for various diseases, including hypertension, it has been demonstrated that changes in biophysical membrane parameters are closely associated to the pathology of these disorders (3, 4). In this context, we recently demonstrated that hypertensive patients on a Mediterranean-style diet containing virgin olive oil showed a reduction of elevated blood pressure, which correlated with changes in membrane lipid composition and which was linked with plasma membrane structural properties, such as an increase in phosphatidylethanolamine (PE) lipid class and a higher propensity to form a nonlamellar H_{II} structure of reconstituted plasma membranes (5). This is an important finding, because it has been shown that PE lipids are able to modulate peripheral protein-membrane interactions via their H_{II} phase propensity (6). Moreover,

Abbreviations: 2MOA, 2-methyloleic acid; 2MSA, 2-methylstearic acid; 2OHOA, 2-hydroxyoleic acid; 2OHSa, 2-hydroxystearic acid; cVcc, *cis*-vaccenic acid; DEPE, 1,2-diacyl-*sn*-glycero-3-phosphoethanolamine; EA, elaidic acid; EFA, essential fatty acid; FA, fatty acid; GBSA, generalized born surface area; H_{II}, inverted hexagonal phase; L_β, gel lamellar phase, L_α, liquid-crystalline lamellar phase; MD, molecular dynamics; MUFA, monounsaturated fatty acid; OA, oleic acid; PE, phosphoethanolamine; PeA, palmitelaidic acid; PL, phospholipid; PoA, palmitoleic acid; PUFA, polyunsaturated fatty acid; rdf, radial density function; SA, stearic acid; SAXS, small-angle X-ray scattering; T_H, liquid lamellar-to-inverted hexagonal phase transition temperature; T_m, gel-to-liquid lamellar phase transition temperature; WAXS, wide-angle X-ray scattering.

¹A. Cordoní and J. Prades contributed equally to this work.

²To whom correspondence should be addressed.
e-mail: francisca.barcelo@uib.es

This work was supported by the following grants: II-05-05IEC from Deutsches Elektronen-Synchrotron DESY; Hasylab (Hamburg, Germany) from the IHP-Contract HPRI-CT-2001-00140 of the European Commission; PI051340 from the Spanish Plan Nacional de Investigación Científica, Desarrollo e Innovación Tecnológica, Instituto de Salud Carlos III-Fondo de Investigación Sanitaria; and AAEE0024/08 from the Conselleria d'Economia, Hisenda i Innovació de les Illes Balears both cofinanced by FEDER, BFU2007-61071/BCM (Ministerio de Educación y Cultura, Spain). The Spanish Ministry of Science and Technology supported this work through grant SAF2008-04943-C02-01. O.V. is supported by the Spanish I3 Program for intensification of scientific research.

Manuscript received 13 October 2009 and in revised form 19 November 2009.

Published, JLR Papers in Press, November 19, 2009

DOI 10.1194/jlr.M003012

Copyright © 2010 by the American Society for Biochemistry and Molecular Biology, Inc.

This article is available online at <http://www.jlr.org>

Journal of Lipid Research Volume 51, 2010 1113

alteration of membrane FA composition is able to influence pivotal elements of important signaling transduction pathways, which finally control vital physiological functions, such as cardiovascular parameters (4, 7). Thus, if cell functions are altered when membrane lipid composition changes, then modulation of biophysical membrane properties by administration of appropriate FAs might be a strategy to revert disease status. This novel pharmacological approach has recently been introduced as membrane-lipid therapy (8). An important step to a rational design of new lipid molecules with pharmacological activity is a comprehensive study of the differential effects of closely related FAs on the structural properties of phospholipid membranes.

The asymmetric distribution of PE phospholipids and the relatively high proportion of this lipid in the cytosolic leaflet of the mammalian plasma membrane (~30%) indicates that PE should have a great functional relevance. In fact, PE lipids have an intrinsic propensity to segregate forming nonlamellar H_{II} structures in vitro (9), and some special features were attributed to H_{II}-prone phospholipids, such as the functional control of membrane proteins and the structural organization inside cells (10–12). On the other hand, FAs incorporated in phospholipids or present in the membrane in their unesterified form are able to modulate the structure of model PE membranes by interacting specifically with the latter (13, 14). This is also true for synthetic fatty acids. 2-Hydroxyoleic acid (2OHOA), a synthetic derivative of the naturally occurring oleic acid, induced the formation of H_{II} structures in model membranes (15). In vivo, this observation was paralleled by an alteration of the membrane lipid composition which was related to the observed increase of G proteins in the plasma membrane of 2OHOA-treated animals (12, 16). Moreover, 2OHOA showed a strongly enhanced antihypertensive action in this animal model of hypertension (17, 18), thus demonstrating the viability of this new pharmacological approach.

In the present study, we explore the effect of the structural parameters acyl chain length, double bond position, and stereochemical properties of series of FAs (Fig. 1) on the structural properties of PE model membranes, using X-ray diffraction and MD simulations. Our study comprises a series of both natural and synthetic FAs, which are described below. OA and SA (18:0) are the major lipid components of animal tissues. Palmitoleic acid (*cis*-16:1n7, PoA) is the delta-9 desaturase product of palmitic acid (16:0) and a minor component of most lipid classes, generally found in higher concentrations in the liver. *Cis*-vaccenic acid (*cis*-18:1n7, cVcc) is the direct elongation product of palmitoleic acid and an essential fatty acyl-component of cardiolipin. Palmitelaidic (*trans*-16:1n7, PeA) and EA are dietary *trans*-FAs, which have received growing attention because of their negative influence on cardiovascular health (19). Four additional synthetic FAs are included to elucidate the effect of chemical modifications on membrane structural parameters: 2-methyloleic, 2-hydroxyoleic, 2-methylstearic, and 2-hydroxystearic FAs.

MATERIALS AND METHODS

Materials

The FAs palmitoleic (PoA), palmitelaidic (PeA), oleic (OA), elaidic (EA), *cis*-vaccenic (cVcc), stearic (SA), and 2-methylstearic acid (2MSA), as well as N-(2-hydroxyethyl) piperazine-N'-(2-ethanesulfonic acid) sodium salt (HEPES) were obtained from Sigma-Aldrich (Madrid, Spain). 2-hydroxystearic acid (2OHSa) was purchased from Larodan (Malmö, Sweden), and 1,2-dielaidoyl-*sn*-glycero-3-phosphoethanolamine (DEPE) and 2-hydroxyoleic acid (2OHOA) were purchased from Avanti Polar Lipids, Inc. (Alabaster, AL). 2-methyloleic acid was synthesized as described elsewhere (20) with a purity of 90%. Lipids were stored under argon at –80°C.

Model membrane preparation

Multilamellar lipid vesicles (MLV; 15% w/w) were prepared in 10 mM HEPES, 100 mM NaCl, 1 mM EDTA, pH 7.4 (HEPES buffer). Lipid mixtures were hydrated in the presence or absence of FAs at the specified molar ratio, homogenized with a pestle-type minihomogenizer (Sigma) and vortexed until a suspension was obtained. The suspensions were then submitted to five heating and cooling cycles (heating to 70°C and cooling to 4°C) and equilibrated prior to data acquisition, as previously reported (13).

X-ray diffraction

Small- and wide-angle synchrotron radiation X-ray scattering data (SAXS and WAXS) were collected simultaneously on the Soft Condensed Matter beamline A2 of Hasylab at the storage ring DORIS III of the Deutsches Elektronen Synchrotron (DESY) using standard procedures. Samples were heated from 27°C to 75°C and then cooled to 27°C at a scan rate of 1°C/min. Data collection was performed as described before (13).

Molecular dynamics simulations

All computer simulations were performed using the GRO-MACS 3.3.2 package (21). Molecular dynamics (MD) simulations were performed at 323 K (above the L β -to-L α phase transition and below the temperature of L α and H_{II} coexistence) using periodic boundary conditions and a time step of 4 fs. The temperature was kept constant using separate thermostats for lipids, water, and ions with a time constant of 0.1 ps. The pressure in the three coordinate directions was kept at 0.1 MPa by independent Berendsen barostats using a time constant of 1.0 ps. Lennard-Jones interactions were computed with a cutoff of 10 Å, and electrostatic interactions were treated with the Particle Mesh Ewald (PME) procedure.

In a first step, a box containing 216 DEPE lipids arranged in a bilayer, more than 10,000 water molecules, 28 sodium, and 28 chloride ions was constructed as described in a previous study (22) and simulated for 200 ns. In a second step, boxes for DEPE:FA systems were constructed by replacing 5 lipids on each leaflet by FAs and removing 6 additional lipids. This procedure allows simulating systems with the desired DEPE:FA molecular ratio of 20:1. Similar simulations working with phospholipid/FA systems have recently been reported (23–25). To preserve electroneutrality, 10 water molecules were replaced by 10 additional Na⁺ ions. Each system was energy minimized and subsequently, subjected to 200 ns MD simulations at 323 K following the protocol previously described in various reports (22, 26, 27). For each trajectory, the first 100 ns were considered as equilibration period and were not included in the analysis.

In the absence of specific force field parameters for DEPE lipids available, a combination of DPPC (28) and POPE parameters (taken from Tieleman's group [http://moose.bio.ucalgary.ca/])

Fatty Acids	Abbr. ¹	Nomenclature IUPAC	Nutritional
	PoA	(9Z)-hexadec-9-enoic acid	16:1(n-7)
	PeA	(9E)-hexadec-9-enoic acid	16:1(n-7)
	OA	(9Z)-octadec-9-enoic acid	18:1(n-9)
	2MOA	(9Z)-2-methyloctadec-9-enoic acid	18:1(n-9)
	2OHOA	(9Z)-2-hydroxyoctadec-9-enoic acid	18:1(n-9)
	EA	(9E)-octadec-9-enoic acid	18:1(n-9)
	SA	octadecanoic acid	18:0
	2MSA	2-methyloctadecanoic acid	18:0
	2OHSA	2-hydroxyoctadecanoic acid	18:0
	cVcc	(11Z)-octadec-9-enoic acid	18:1(n-7)

Fig. 1. Chemical structure of the fatty acids. 2MOA, 2-methyloleic acid; 2MSA, 2-methylstearic acid; 2OHOA, 2-hydroxyoleic acid; 2OHSA, 2-hydroxystearic acid; cVcc, *cis*-vaccenic acid; EA, elaidic acid; OA, oleic acid; PeA, palmitelaidic acid; PoA, palmitoleic acid.

was used. The area per DEPE lipid is not known experimentally, although it is reasonable to expect to be similar to DPPE, for which it has been determined at two different temperatures (29). Preliminary simulations (data not shown) employing these parameters revealed that DEPE bilayers were half way to the gel phase, in agreement with recent simulations of DPPE membranes (30, 31). This suggested the necessity to introduce a correction for PE lipids. Scaling ϵ Lennard-Jones parameters for the acyl carbons by a factor of 3/4 provided an area compatible with all the observations above. FA topologies were generated by PRODRG 2.5 β server (32), whereas the parameters were taken by analogy to the lipids force field (28). All FAs were modeled as negatively charged according to the results of our previous report (15). The apparent pKa of FAs is typically about 7 when incorporated in the bilayer of a phospholipid vesicle, although the specific value varies depending upon the environment (33, 34).

RESULTS

X-ray diffraction study

We addressed the effect of FAs on the structural properties of model DEPE membranes. The sequence of diffraction patterns collected showed defined phase transitions that allowed unequivocal characterization of the L_{β} , L_{α} and H_{II} phases, and their respective lattice pa-

rameters (**Fig. 2** and **Table 1**). X-ray heating scans of DEPE:FA (20:1, mol:mol) mixtures showed a L_{β} phase up to 38°C–40°C with a repeat distance value of 6.5–6.7 nm similar to the value shown for DEPE alone. A single L_{α} phase was present in the range from 38–39°C to 51–57°C, with a repeat distance value of 5.4–5.5 nm at 40°C, which decreased linearly with temperature (compressibility factor ~ -0.013 nm/°C). Above these temperatures, the L_{α} phase developed into a binary system, where L_{α} and H_{II} phases coexisted in a range that depended on each FA. Finally, a single H_{II} phase appeared with a repeat distance value of ~ 6.4 nm at 72°C and a constant compressibility factor in the range from -0.020 to -0.025 nm/°C. The main effect of FAs on membrane structure was to induce the formation of a H_{II} phase at a lower temperature than DEPE alone, despite a stabilization of the coexisting L_{α} + H_{II} phases. X-ray measurements did not highlight the differences in the interaction between DEPE and FAs, a detail that was further investigated by MD simulations.

Molecular dynamics study

Analysis of the MD trajectories of the different DEPE:FA systems permits the characterization of the molecular arrangement of each FA in the DEPE bilayer at the atomistic

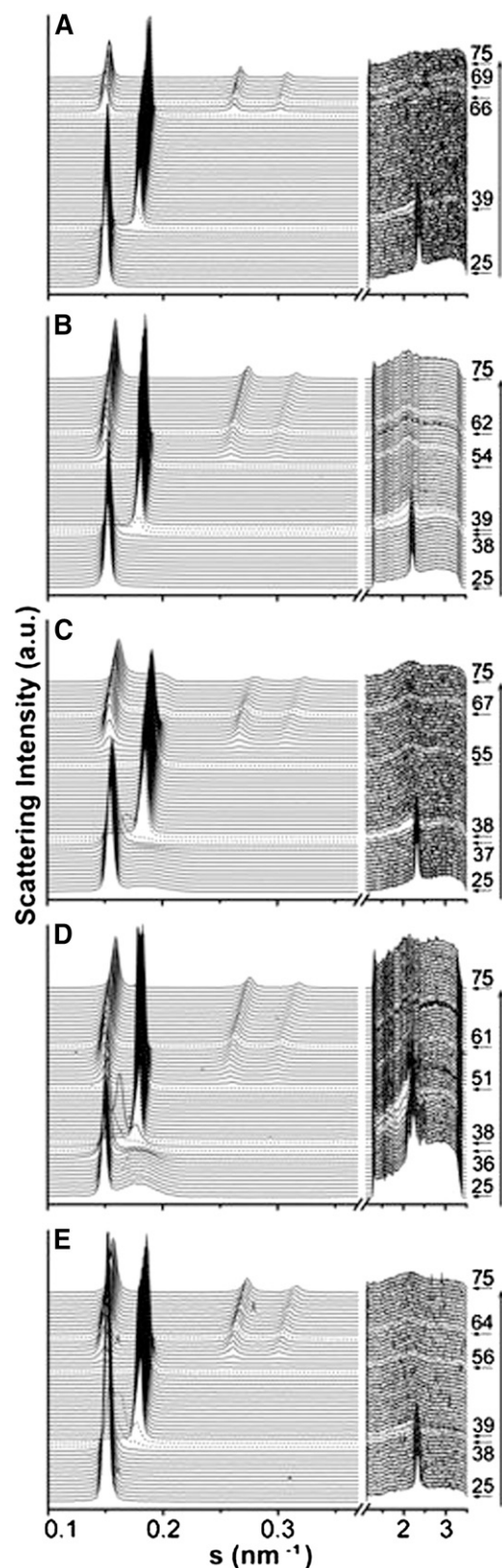


Fig. 2. Linear plots of the X-ray scattering patterns. (A) DEPE alone and in presence of the fatty acids; (B) OA; (C) 2OHOA; (D) 2MOA; and (E) cVcc at a molar ratio 20:1. The sequence of the patterns was acquired with a scan rate of 1°C/min. Successive diffraction patterns were collected for 15 s each minute. Only the heating sequence from 27°C to 72°C is shown. The L_{β} phase was identified by a sharp and intense SAXS reflection ($s \approx 0.15 \text{ nm}^{-1}$),

level, as well as the identification of specific interactions. According to the system design (see “Materials and Methods”), the two leaflets in the DEPE bilayer can be considered as equivalent, and therefore, the analysis presented in this report is an average of the two layers. Whenever possible, the analysis of the systems is displayed in three groups corresponding to the type of FA present: (1) OA series - OA, 2OHOA and 2MOA-; (2) SA series - SA, 2OHSA and 2MSA-; and (3) the remaining FAs not substituted at carbon -2 of the acyl chain (PeA, PoA, EA, and cVcc).

FA positioning in the membrane. **Fig. 3** displays snapshots of equilibrated DEPE:FA systems showing the disposition of the FAs in the bilayer for each of the three members the OA series. The average position of each type of FA within a DEPE layer was monitored using the atom density distribution along the axis perpendicular to the bilayer plane (**Fig. 4A**). Decomposition of the total atom density distribution into its components allows us to assign the distinct features of each FA. The density of the DEPE molecules exhibits a maximum in the region 0.5–2.5 nm relative to the bilayer center with a peak at 2.1 nm that corresponds to the head groups (phosphate and ethanolamine). The density of water suggests that molecules penetrate up to 1.75 nm with an interfacial region up to 3 nm that overlaps with the density provided by the polar head groups (35).

All FAs occupy a region between the bilayer center and up to 3.0 nm with differences depending on their specific structural features. In the OA series, the atom density distribution of 2OHOA is shifted toward the water phase when compared with OA, and in the opposite direction in the case of the 2MOA. 2OHOA and (to a lesser extent) 2MOA systems exhibit a peak at 2.0–2.1 nm (at the same position as the maximum in the profile showed by DEPE alone), which originates from the additional contribution of the hydroxyl/methyl group at position C2. A similar trend is found within the SA series. The remaining FAs with 18 carbons (EA and cVcc) showed similar profiles to OA and SA. On the contrary, FAs with shorter chains (PoA and PeA) exhibited a much smaller density in the region close to the bilayer center, indicating that 16 carbons are not enough to go across the whole DEPE layer.

Fig. 4B displays density distributions for FA carboxyl carbons along the axis perpendicular to the bilayer plane. **Table 2** shows the (time and system) average positions, which provides a measure of the relative distances with the ethanolamine moieties. It can be seen that there is a small difference both in the amplitude of the peak and also in

accompanied by a well-defined reflection in the WAXS region. The L_{α} phase was identified by a single peak of reflection ($s \approx 0.19 \text{ nm}^{-1}$), with a very good signal-to-noise ratio. The L_{β} -to- L_{α} phase transition was defined by the vanishing peak in the WAXS region of the pattern. The appearance of three diffraction orders in the SAXS region with a d-spacing ratio of $1:1/\sqrt{3}:1/\sqrt{4}$ indicated the formation of the H_{II} phase. 2MOA, 2-methyloleic acid; 2OHOA, 2-hydroxyoleic acid; cVcc, *cis*-vaccenic acid; DEPE, 1,2-diacyl-sn-glycero-3-phosphoethanolamine; SAXS, small-angle synchrotron radiation; WAXS, wide-angle synchrotron radiation.

TABLE 1. Structural properties of DEPE:FA mixtures

Sample Composition	$\delta d/\delta T$ (L_α) (nm/ $^{\circ}\text{C}$) ^a	$\delta d/\delta T$ (H_{II}) (nm/ $^{\circ}\text{C}$) ^a	ΔT_{L_α} ($^{\circ}\text{C}$) ^b	d_{L_α} (nm) ^c	$d_{H_{II}}$ (nm) ^c
DEPE	-0.012	-0.021	(38) 40 – 66 (69)	5.60	6.59
DEPE:PoA	-0.013	-0.023	(39) 40 – 57 (64)	5.58	6.41
DEPE:PeA	-0.013	-0.022	(38) 39 – 56 (62)	5.57	6.39
DEPE:OA	-0.009	-0.023	(38) 39 – 54 (62)	5.52	6.35
DEPE:2MOA	-0.012	-0.025	(36) 38 – 51 (61)	5.60	6.34
DEPE:2OHOA	-0.011	-0.019	(37) 38 – 55 (67)	5.47	6.37
DEPE:EA	-0.013	-0.022	38 – 57 (59)	5.43	6.29
DEPE:SA	-0.013	-0.027	(39) 42 – 62 (65)	5.70	6.53
DEPE:2MSA	-0.012	-0.026	(39) 40 – 59 (63)	5.68	6.43
DEPE:2OHSa	-0.012	-0.022	(39) 40 – 64 (69)	5.63	6.57
DEPE:cVcc	-0.013	-0.024	(38) 39 – 56 (64)	5.58	6.46

DEPE:FA mixtures, 20:1 (mol:mol). The angular coefficient of the interplanar distance dependence on the temperature ($\delta d/\delta T$) < 0 indicates a compression process. 2MOA, 2-methyloleic acid; 2MSA, 2-methylstearic acid; 2OHOA, 2-hydroxyoleic acid; 2OHSa, 2-hydroxystearic acid; cVcc, *cis*-vaccenic acid; DEPE, 1,2-diacyldoyl-*sn*-glycero-3-phosphoethanolamine; EA, elaidic acid; FA, fatty acid; H_{II} , inverted hexagonal phase; L_β , gel lamellar phase, L_α , liquid-crystalline lamellar phase; OA, oleic acid; PeA, palmitelaidic acid; PoA, palmitoleic acid; SA, stearic acid.

^a The compressibility factor of the L_α phase was linear in the single- or two-phase regions. Single H_{II} phases also had linear compressibility factor. The temperature range where the L_α phase was observed is shown in ΔT_{L_α} .

^b The parenthesis indicates the temperature limit of the L_α phase in a two-phase region. Values on the left correspond to $L_\beta + L_\alpha$ and on the right to $L_\alpha + H_{II}$ temperature range coexistence.

^c d_{L_α} at 40°C and $d_{H_{II}}$ at 72°C.

the relative positioning. 2OHOA exhibits a wider distribution, and it is shifted toward the solvent when compared with the remaining FAs. Comparison between different nonsubstituted FA suggests that there is a small effect in the distribution of carboxyl carbons due to the double bond position or configurations. Remarkably, SA and OA FAs exhibit a narrower distribution than EA and cVcc. PeA and PoA have intermediate distributions between these FAs (data not shown). Overall, the present data indicates differences in relative carboxylate positions and average density distributions depending on the FA.

Effect of the fatty acid on lipid order. The lipid bilayer order was assessed by measuring its average thickness (com-

puted from the distance between the planes defined by the phosphate groups in each layer) and the average area per lipid (Table 3). The different DEPE:FA systems exhibit average thickness ranging $4.90\text{--}4.92 \pm 0.02$ nm, slightly smaller than the value computed without FAs of 4.93 ± 0.02 nm. Comparatively, theoretical estimates obtained from simulations are $\sim 0.5\text{--}0.8$ nm smaller than the experimental data of the lamellar repeat distance (d_{L_α}) in excess of water obtained by X-ray diffraction experiments (see Table 1). Such difference can be attributable to the water layer between lamellar repeats. The area per lipid was estimated as described elsewhere (35) by considering the volume of each FA, the total system area and system volume, and the solvent volume. The computed average area per

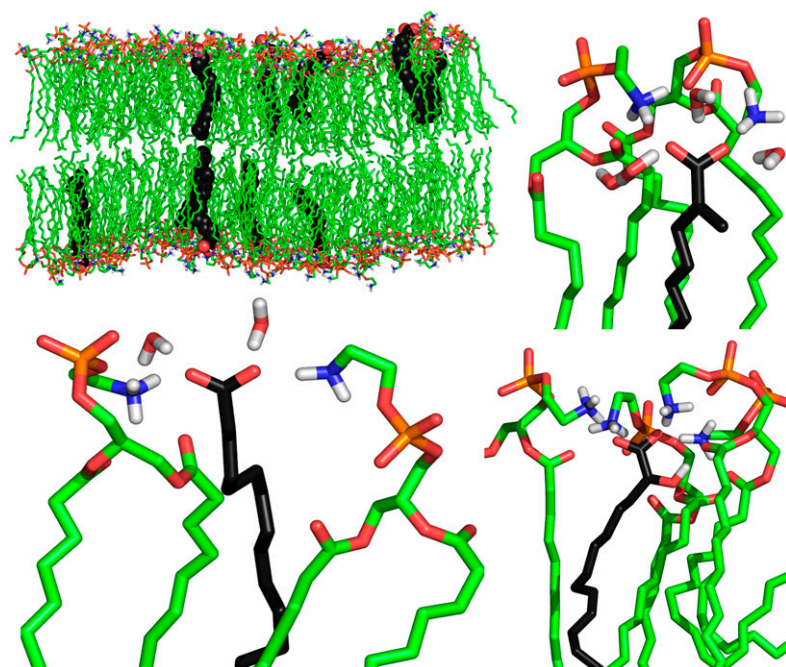


Fig. 3. Snapshots of representative DEPE:FA systems taken from the simulations: DEPE:OA system (top-left), details of single OA (bottom-left), 2MOA (top-right) and 2OHOA (bottom-right) FA showing the H-bond interactions with neighboring lipids and water molecules. DEPE acyl chains are colored in green and FA acyl chains in black. The polar head of each molecule is colored by atom type: blue, nitrogen; orange, phosphorous; red, oxygen. 2MOA, 2-methyloleic acid; 2OHOA, 2-hydroxyoleic acid; DEPE, 1,2-diacyldoyl-*sn*-glycero-3-phosphoethanolamine; FA, fatty acid.

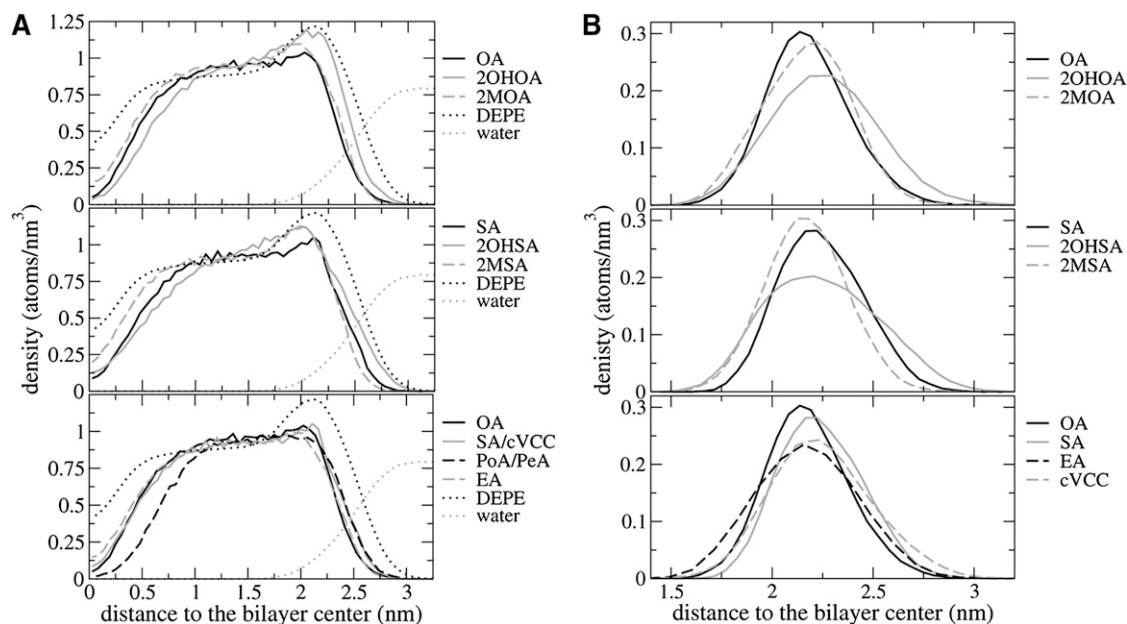


Fig. 4. (A) Atom density distribution of the FA along the axis perpendicular to the bilayer plane. Fatty acid series: OA (top), SA (middle) and non-C2-substituted (bottom). The bilayer center is considered as the reference point. The distribution corresponding to DEPE and water are shown as a reference in a reduced scale (divided by 40) for an easier comparison. (B) Analogous density distributions for the carboxylate carbon only. 2MOA, 2-methyloleic acid; 2MSA, 2-methylstearic acid; 2OHOA, 2-hydroxyoleic acid; 2OHSa, 2-hydroxystearic acid; cVcc, *cis*-vaccenic acid; DEPE, 1,2-dielaidoyl-*sn*-glycero-3-phosphoethanolamine; EA, elaidic acid; PeA, palmitelaidic acid; PoA, palmitoleic acid; SA, stearic acid.

lipid does not change significantly from one system to another ($0.512\text{--}0.516\text{ nm}^2$). On the other hand, an average area of 0.517 nm^2 for free-FA system was found, in reasonable agreement with the available experimental measurements (29). Compared with recent simulations of DOPC/FA systems (25), the present results indicate that the stronger interactions between PE groups give a smaller decrease in the area per lipid in presence of FAs. Thus, the incorporation of FAs to the lipid bilayer has a small effect on the L_α phase order in DEPE:FA systems at 20:1 molar ratio, in agreement with the experimental data reported.

TABLE 2. Average localization of FA carboxylate groups relative to the membrane in the different systems

System	COO_{FA} (nm)	$\text{P}_{\text{DEPE}}\text{-COO}_{\text{FA}}$ (Å)	$\text{N}_{\text{DEPE}}\text{-COO}_{\text{FA}}$ (Å)
DEPE:OA	2.12	3.0	1.7
DEPE:2OHOA	2.25	1.9	0.3
DEPE:2MOA	2.22	2.2	0.9
DEPE:SA	2.29	1.6	0.4
DEPE:2OHSa	2.15	3.1	2.0
DEPE:2MSA	2.15	3.1	1.8
DEPE:EA	2.16	3.0	1.5
DEPE:cVcc	2.20	2.6	1.7
DEPE:PeA	2.24	2.1	0.5
DEPE:PoA	2.19	2.7	1.0

COO_{FA} is the average distance between FA carboxylate carbons and the bilayer center ($\text{SD} < \pm 0.02$). $\text{P}_{\text{DEPE}}\text{-COO}_{\text{FA}}$ and $\text{N}_{\text{DEPE}}\text{-COO}_{\text{FA}}$ represent the relative distances to the average positions for DEPE phosphorus and nitrogen atoms. 2MOA, 2-methyloleic acid; 2MSA, 2-methylstearic acid; 2OHOA, 2-hydroxyoleic acid; 2OHSa, 2-hydroxystearic acid; cVcc, *cis*-vaccenic acid; DEPE, 1,2-dielaidoyl-*sn*-glycero-3-phosphoethanolamine; EA, elaidic acid; FA, fatty acid; H_{II} , inverted hexagonal phase; L_β , gel lamellar phase; L_α , liquid-crystalline lamellar phase; OA, oleic acid; PeA, palmitelaidic acid; PoA, palmitoleic acid; SA, stearic acid.

The correlation between critical phosphorus (P) and nitrogen (N) atoms in DEPE molecules was analyzed by computing radial density distribution function (rdf) for all possible atom-atom combinations. As shown in **Fig. 5**, all DEPE:FA systems exhibit an increase in the value of the maximum of the N-N function with regard to DEPE simulation without FAs, due to the fact that the negative charge of the FAs allows ethanolamine nitrogens to be closer to each other. This property indicates that FAs alter the lateral order of DEPE bilayers, which affects the hexagonal H_{II} phase transition. Furthermore, it seems reasonable to hypothesize that a larger effect could be observed for larger DEPE:FA ratios. Conversely, the computed rdf functions for P-P and P-N pairs exhibit a peak centered at 0.53 nm and at 0.40 nm, respectively, in all systems analyzed independently of the presence of different FAs (data not shown), indicating no differences from one system to another.

DEPE-FA interactions. To evaluate the interactions between FA carboxyl groups and DEPE lipids, four additional rdfs were calculated for all systems simulated, including those of the carbon atom of the FA carboxyl group and different DEPE atoms: ethanolamine nitrogen [$\text{C}(\text{COO})_{\text{FA}}\text{-N}_{\text{DEPE}}$]; phosphorous atom [$\text{C}(\text{COO})_{\text{FA}}\text{-P}_{\text{DEPE}}$]; and the carbonyl oxygens of the *sn*-1 and *sn*-2 chains [$\text{C}(\text{COO})_{\text{FA}}\text{-C}(\text{O})_{\text{DEPE}}$]. Rdfs corresponding to the OA series are shown in **Fig. 6** as representative cases. Similar trends are observed for all DEPE:FA systems studied. There is a strong $\text{C}(\text{COO})_{\text{FA}}\text{-N}_{\text{DEPE}}$ correlation, whereas $\text{C}(\text{COO})_{\text{FA}}\text{-P}_{\text{DEPE}}$ and $\text{C}(\text{COO})_{\text{FA}}\text{-C}(\text{O})_{\text{DEPE}}$ present a much weaker correlation. It can be seen that the rdf for $\text{C}(\text{COO})_{\text{FA}}\text{-N}_{\text{DEPE}}$ exhibits a sharp, double peak with two maxima at 0.33 and 0.36

TABLE 3. Structural parameters of DEPE:FA systems

System	Thickness _{P-P} (nm)	area _{DEPE} (nm ²)	−Δpotential (mV)
DEPE:OA	4.90	0.512	31
DEPE:2OHOA	4.91	0.512	36
DEPE:2MOA	4.92	0.512	20
DEPE:SA	4.90	0.516	51
DEPE:2OHSa	4.90	0.514	43
DEPE:2MSA	4.90	0.516	0
DEPE:EA	4.91	0.515	74
DEPE:cVcc	4.91	0.515	43
DEPE:PeA	4.92	0.513	8
DEPE:PoA	4.91	0.513	4
DEPE	4.93	0.517	0

Bilayer thickness was computed from the average distance between phosphate planes (std. dev. $< \pm 0.02$). The area per lipid (SD $< \pm 0.007$) was computed as in reference (35). The variation of the electrostatic potential was calculated taking DEPE electrostatic potential as reference (795 mV). 2MOA, 2-methyloleic acid; 2MSA, 2-methylstearic acid; 2OHOA, 2-hydroxyoleic acid; 2OHSa, 2-hydroxystearic acid; cVcc, *cis*-vaccenic acid; DEPE, 1,2-diacyldiacyl-*sn*-glycero-3-phosphoethanolamine; EA, elaidic acid; FA, fatty acid; OA, oleic acid; PeA, palmitelaidic acid; PoA, palmitoleic acid; SA, stearic acid.

nm (Fig. 6A). This pattern suggests the existence of at least two groups of interactions, one closer than the other. Remarkably, the area under the peak is smaller for 2OHOA than for the remaining FAs of the OA series, indicating that the hydroxyl group diminishes the magnitude of the correlation.

The $C(\text{COO})_{\text{FA}}\text{-P}_{\text{DEPE}}$ rdf (Fig. 6B) exhibits a rough profile with a maximum at about 0.6 nm for all the systems. Since the carboxyl and phosphate groups are both negatively charged, this effect must be considered a consequence of the strong correlation with the neighboring N_{DEPE} atom. However, it can be seen that DEPE:2OHOA system exhibits a tail at short distances, reflecting the existence of additional interactions between the 2-hydroxyl groups with DEPE phosphate oxygens. The same effect is observed for the DEPE:2OHSa system (data not shown). Regarding the $C(\text{COO})_{\text{FA}}\text{-C}(\text{O})_{\text{DEPE}}$ rdf (Fig. 6C), there is a maximum correlation at 0.45 nm both for the *sn*-1 and *sn*-2 chains. For all systems except 2OHOA and 2OHSa, the correlation is larger for the *sn*-1 chain than for the *sn*-2. The larger difference is observed for 2MOA and 2MSA, pointing to the preference of FAs to interact with DEPE ethanolamine groups from the side of the *sn*-1 chain, and more importantly, that this can be modulated by the substitution at position C2.

An analysis of hydrogen bond interactions between FA carboxyl and DEPE ethanolamine groups was also undertaken (Table 4). For 2OHOA and 2OHSa, the hydrogen binding hydroxyl group was also considered. We identified a large network of H-bond and charge interactions in the interfacial region of the membrane involving DEPE lipids, FA, water molecules, and ions. They provide strong interactions that are probably responsible for stabilizing the bilayer in the L_α phase. Each FA forms roughly two H-bonds with DEPE donors/acceptors, with the specific numbers ranging between 1.8 and 2.5 depending on the FA type, considering a cutoff of 0.3 nm. Excluding C2-substituted FAs, the number of interactions decreases as $\text{SA} > \text{OA} > \text{PoA} > \text{EA} > \text{PeA} > \text{cVcc}$, indicating a dependence on

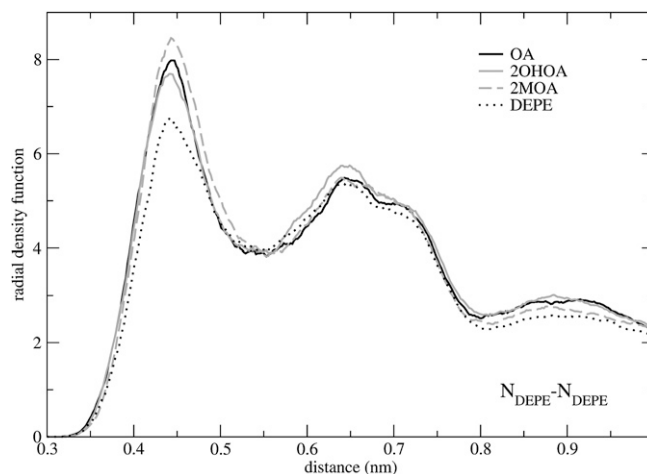


Fig. 5. Radial density functions between DEPE nitrogen head-group atoms. 2MOA, 2-methyloleic acid; 2OHOA, 2-hydroxyoleic acid; DEPE, 1,2-diacyldiacyl-*sn*-glycero-3-phosphoethanolamine; OA, oleic acid.

the presence of a double bond, its position and configuration, and the acyl chain length. Interestingly, the *cis* configuration always induced a higher number of DEPE-FA hydrogen bond interactions than the *trans* (PoA vs. PeA; OA vs. EA).

Among OA series, the number of interactions decrease as $2\text{OHOA} > 2\text{MOA} > \text{OA}$, whereas in SA series, it follows the order $2\text{MSA} > 2\text{OHSa} > \text{SA}$. The results suggest that a bulkier FA head (a C2 substitution in the acyl chain) enhances the number of interactions, especially for the SA series. Moreover, the specific trends seem to be related to the different ability of each series to interact with the aliphatic chains of DEPE lipids, which result in a different relative positioning as discussed below. The presence of FA molecules within DEPE lipids reduced the number of DEPE-DEPE H-bonds per molecule from 2.0 to 1.8, considering a maximum interatomic distance of 0.4 nm. The number of DEPE-water H-bonds also decreased from 5.7 up to 4.7 interactions per phospholipid, considering the same cutoff owing to the different localization of the FA carboxyl group in the polar region of the bilayer. The number of H-bonds was 1–2 units smaller than in DOPC/FA systems (25) due to the existence of H-bonds between PE groups. The presence of the FA hydroxyl group gives a small increase in the number of direct interactions with DEPE lipids (10%) but allows the possibility to form water-mediated interactions, providing an additional increase in the number of hydrogen bonds with water molecules.

Electrostatic features of the lipid membrane. Table 3 displays the computed electrostatic potentials (measured from the bilayer center to the water interface) for all simulated systems. The values were obtained by integrating charge densities twice according to the one-dimensional Poisson equation (36). A DEPE bilayer without FAs exhibits a potential of -795 mV, which originates mainly from the macroscopical charge distribution created from the sum of individual phosphorus-nitrogen (P-N) dipoles. It is reason-

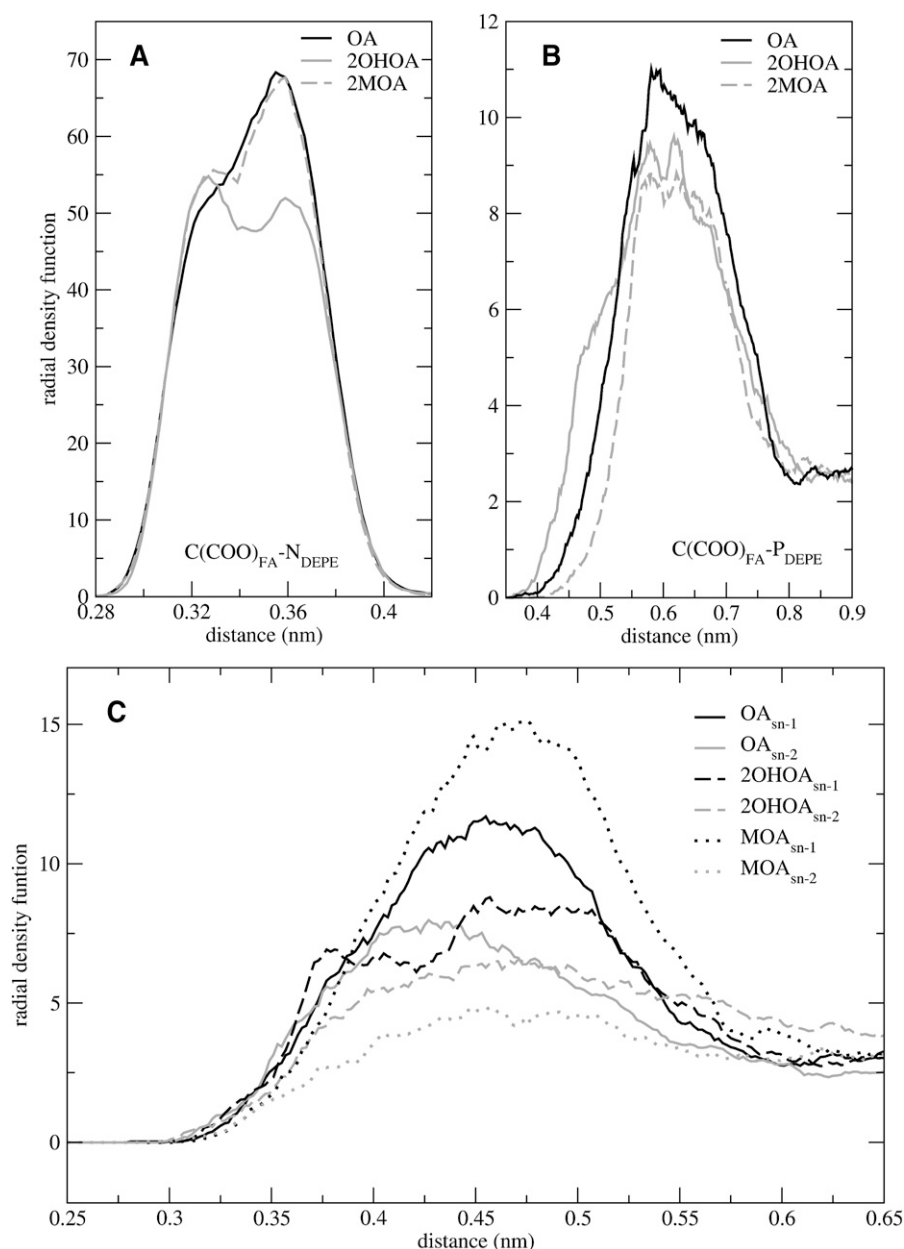


Fig. 6. Radial density functions between the carbon atom of the FA-carboxylate group and nitrogen (A); phosphorus (B); and carbonyl atoms of DEPE (C). 2MOA, 2-methyloleic acid; 2OHOA, 2-hydroxyoleic acid; DEPE, 1,2-dielaidoyl-*sn*-glycero-3-phosphoethanolamine; FA, fatty acid; OA, oleic acid.

able to expect various contributions to this potential including the P-N dipole, but also the degree of water polarization and the presence of bound ions. In DEPE:FA systems there is an additional contribution due to the FA carboxyl group. The total electrostatic potential computed for DEPE:FA systems are the same or smaller than that computed for DEPE alone (with a maximum decrease of 74 mV). The specific trends that can be observed in the table are not fully understood, although they indicate the existence of distinct charge distributions of the different system components within the interfacial region of the membrane that tend to compensate each other.

Figure 7 displays the number density distributions for atoms of the functional groups in DEPE:2OHOA and

DEPE:OA systems, as well as the charge densities provided by the different molecules. For comparison, the specific average positions for the carboxyl carbons in these and the remaining systems studied are shown in Table 2, together with the relative distances to phosphorus and nitrogen DEPE atoms. The results shown are qualitatively similar to the remaining systems studied. It can be seen that the density of DEPE phosphorus atoms is maximal at 2.4 nm whereas the density for nitrogens exhibits the maximum at 2.3 nm. This generates a dipole whose (time and system) average orientation is 6.5° measured from the bilayer plane and facing toward the bilayer in a system without FAs. This value is in good agreement with previous results of PE bilayers (30) and differs from those of PCs, where

TABLE 4. H-bond interactions between FAs, DEPE lipids, and water molecules

	DEPE-FA <0.3 nm	FA-H ₂ O <0.4 nm	DEPE-H ₂ O <0.4 nm	DEPE-DEPE <0.4 nm
DEPE:OA	2.1	2.6	5.3	1.8
DEPE:2OHOA	2.3 (2.1 ^a)	3.2	4.7	1.8
DEPE:2MOA	2.2	2.8	4.8	1.8
DEPE:SA	2.3	2.5	4.7	1.8
DEPE:2OHSA	2.3 (2.0 ^a)	3.6	5.1	1.8
DEPE:2MSA	2.5	2.1	5.2	1.8
DEPE:EA	1.9	3.0	5.1	1.8
DEPE:cVcc	1.8	3.1	5.2	1.8
DEPE:PeA	1.9	3.1	5.0	1.8
DEPE:PoA	2.1	2.8	5.0	1.8
DEPE	—	—	5.7	2.0
Standard deviation	<±0.2	<±0.5	<±0.2	<±0.06

The values have been normalized either to the number of FA (DEPE-FA and FA-H₂O) or to the number of DEPE lipids (DEPE-H₂O and DEPE-DEPE). 2MOA, 2-methyloleic acid; 2MSA, 2-methylstearic acid; 2OHOA, 2-hydroxyoleic acid; 2OHSA, 2-hydroxystearic acid; DEPE, 1,2-diacyldoyle-*sn*-glycero-3-phosphoethanolamine; EA, elaidic acid; FA, fatty acid; OA, oleic acid; PeA, palmitelaidic acid; PoA, palmitoleic acid; SA, stearic acid.

^a Number of H-bonds excluding -OH group.

the P-N angle is about 15° in the opposite direction, that is, pointing toward the water face (22). DEPE:FA systems exhibit almost the same value for the P-N angle as the DEPE bilayer with the small increase of 0.8–2.6° that can be attributed to a shift in the N_{DEPE} density toward lower distances. This suggests that the extensive network of H-bonds between DEPE molecules allows only a small response of the phospholipid head-group to the negatively charge densities provided by FAs. These results indicate that PE membranes are much poorer charge sensors than PC bilayers (22, 37).

DEPE carbonyl oxygens are located in a much deeper position (2.0–2.1 nm) with the group at the *sn*-2 chain always at a smaller distance than that at *sn*-1. The maximum carboxyl carbon density value corresponds to 2.15 and 2.25 nm for OA and 2OHOA, respectively. Interestingly, the carboxyl groups in the OA system lie close to carbonyl oxygens and overlap with half of the nitrogen density. On the contrary, in the 2OHOA system they are located between carbonyl and phosphate oxygens, almost at the same position than the maximum in the nitrogen density. Moreover, the width of the phosphorus density is slightly smaller for 2OHOA than for OA. The total DEPE charge density shows a rough profile with three maxima and two minima in the OA system and a flatter profile with only one minimum in the case of 2OHOA. It is known from previous studies that the lipid charge distributions in a bilayer are almost compensated by the remaining system components in the interfacial region (22), in this case, water molecules, FAs, and ions. Indeed, water molecules orient cooperatively generating a bimodal charge density, with a maximum at ~2.25 nm and a minimum at ~2.95 nm. Below 3.3 nm, the density of Na⁺ ions is larger than the density of Cl[−], and therefore, they provide an additional contribution to the positive charge density. The Na⁺ density ranges 0.06–0.08 ± 0.02 ions bound per lipid. Some of these ions

also bound to FAs, although the number of both FAs and sodium ions are two small for a quantitative analysis. Remarkably, the binding of ions to the DEPE bilayer without FAs is negligible. Finally, FAs provide a charge density with a single minimum at ~2.2 nm (see Table 2), close to the maxima distance shown by the solvent, sodium ions, and DEPE lipids.

DISCUSSION

The strategy by which the physiology of a cell can be modulated by drugs that interact with membrane lipids or lipid structures has recently been named ‘membrane lipid therapy’ (8). The modulation of the structural and functional properties of cell membranes is a novel pharmacological approach whose molecular basis has not been considered previously but which may be valuable in a variety of human diseases (38). In this context, elucidating the specific interactions of FAs with biomembranes represents the first step toward a design of lipids with potential pharmacological activity. Our study provides a comparative insight into the structural features that alter the molecular location and organization of FAs within DEPE membranes and are able to affect their structural properties.

X-ray diffraction experiments reveal that the main effect of FAs (structurally related to OA) on DEPE membranes is to promote the formation of H_{II}, a nonlamellar phase. In addition, FAs permitted L_α and H_{II} structures to coexist in a wider range of temperatures. The repeat distance of L_α phases did not appear to be sensitive to the presence of structurally related FAs, differing only in the stereochemistry of the double bond, its position in the acyl chain or the chain length (e.g., EA, PoA, PeA, cVcc). When considering these experimental data in conjunction with data from previous studies (13, 14), we conclude that the ability of the FAs to promote H_{II} phase formation in DEPE membranes follows the order 2MOA > OA > 2OHOA, EA, PoA, PeA, cVcc, 2MSA > SA > 2OHSA. To explain the different abilities of FAs to modulate the membrane thermotropic properties, it is necessary to evaluate some structural features, including the degree of FA ionization, the localization of FAs within the membrane, the interactions between FAs and DEPE lipids and water molecules, and possible ordering effects of FAs on bilayers in the L_α phase. The apparent pK_a of FAs is about 7 when incorporated in the bilayer of a phospholipid vesicle. Thus, at physiological pH, FAs could be partially ionized, although the pK_a varies depending upon the environment (33, 34). In previous reports we analyzed the effect of having a net negative charge in 2OHOA and OA within a DEPE matrix, concluding that the extent of FA ionization affected the surface charge density and modulated the number of H-bond interactions in the polar region of the membrane (15, 39). In the present report, the remaining structural features are examined by means of a set of MD trajectories of various DEPE:FA systems simulated in the L_α phase.

For all FAs, the analysis of MD simulations revealed small or negligible effects both in membrane thickness

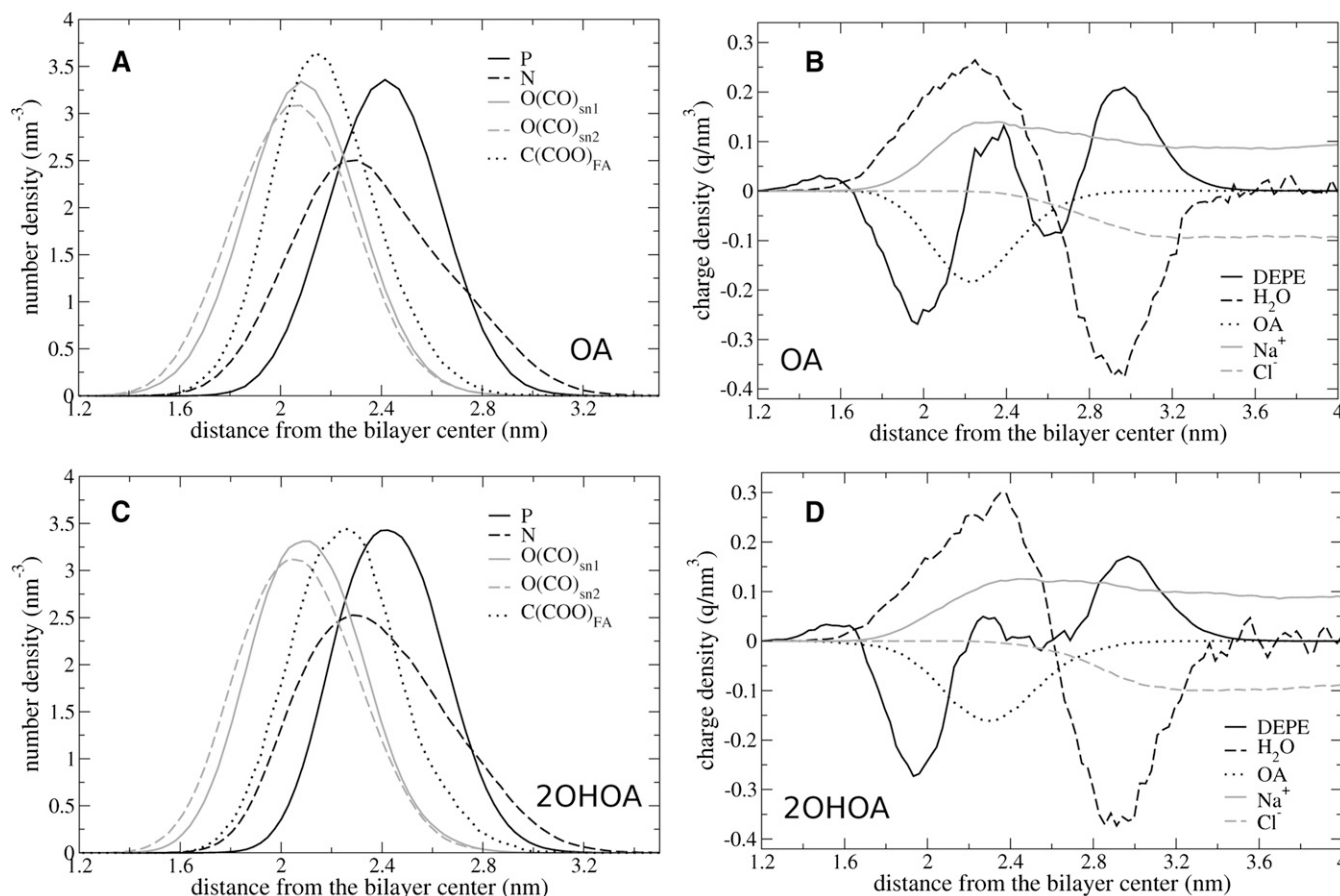


Fig. 7. Average number density distributions of important atoms (A, C) and average charge density distributions for the different species—DEPE lipids, water molecules, FAs, and sodium and chloride ions (B, D)—in DEPE:OA (A, B) and DEPE:2OHOA (C, D) systems. P, N, O(CO)_{snX}, and C(COO)_{FA} indicate phosphate, nitrogen, and carbonyl oxygen atoms in DEPE and FA carboxylates, respectively. DEPE, 1,2-dielaidoyl-*sn*-glycero-3-phosphoethanolamine; FA, fatty acid.


and in the area per DEPE molecule with the presence of FAs in a 20:1 molar ratio, in agreement with the preceding X-ray diffraction experiments. On the contrary, the average density distributions showed the existence of different profiles both for the density of carboxyl carbons and for the acyl chain FA molecule in the axis perpendicular to the membrane plane. These differences are found both in the relative localization and amplitude of the distribution of the carboxyl group within the polar region of the membrane and in the degree of membrane penetration of the FA acyl chain. The chemical group at position C2 strongly modulates the former, whereas the nature of the acyl chain affects mainly the latter. The number of H-bonds, either with DEPE lipids or water molecules, was sensitive to the localization of the FA carboxyl group in the DEPE membrane. C2-substituted FAs exhibit the largest number of DEPE-FA H-bonds as the C2-group provides a larger head group area and, therefore, a more accessible carboxyl group.

Due to the importance of 2OHOA as a hypotensive drug (15), characterizing the differences between DEPE:OA, DEPE:2OHOA, and DEPE:2MOA systems at a molecular level is of large interest. Considering the profile exhibited by OA as a reference, a hydroxyl group at the C2 position (2OHOA) shifts FA atomic densities toward the outer side

of the membrane, whereas a methyl group (2MOA) moves them toward the inner part. On the other hand, the presence of a hydroxyl group provides only a 10% increase in the number of direct interactions with DEPE lipids and gives an additional increase in the number of H-bonds with water molecules. The structural data here presented indicated that the main effect of the C2-substitution is the modulation of the FA density distributions rather than the extent of the H-bond network within the interfacial region of the membrane. Considering the macroscopic “molecular shape model” (9) and assuming a similar molecular geometry for all DEPE:FA systems studied, the primary reason for the 2OHOA, OA, and 2MOA differential effect on the thermotropic behavior of DEPE membranes could be related to the FA effect on the headgroup area at the lipid-water interface, because the acyl chain packing would be similar for all systems. The shift of 2OHOA toward the outer side of the membrane will be associated with a higher optimum headgroup area that could account for the appearance of the L α -to-H_{II} phase transition at higher temperatures and the stabilization of the L α phase, as observed experimentally.

The present study demonstrates that changes in the chemical structure of FAs affect both FA-DEPE and DEPE-DEPE interactions. These are important results, because

not all structural changes in the FA molecules were equally effective in the influence on the membrane structural properties. When trying to extrapolate these findings on biological systems, the results of *in vivo* studies are indicating that the above-mentioned extent of FA-membrane interactions have a correlation to their physiological efficacy. For example, a recent study in rats has demonstrated that saturated SA or *trans*-monounsaturated EA were less effective in reducing blood pressure than the monounsaturated OA (17). In turn, 2OHOA showed a highly increased antihypertensive action in genetically hypertensive rats (18). Moreover, reconstituted plasma membranes from these rats showed a clear shift of their biophysical properties toward a higher propensity to form H_{II} phases, paralleled by a significant increase in the level of unsaturated FAs (16). Although these results do not firmly establish the molecular mechanism of action of 2OHOA, they indicate that the observed alteration of biophysical membrane parameters *in vitro* also occurs *in vivo* and should have pharmacological relevance. In addition, a similar observation regarding body weight homeostasis could be made because neither SA nor EA were able to reduce body weight in rats, while OA showed a slight and 2OHOA a strong lipolytic effect on adipose tissue mass (40).

Summing up, both dietary and synthetic FAs are finally incorporated, at least partially, into cell membranes either as free FAs or in the form of phospholipids. FAs able to affect biophysical properties of cell membranes, in turn will also alter localization and/or function of membrane protein involved in the regulation of cellular processes. For the above reasons, FAs or other lipids could be a tool to modulate pathophysiological conditions via cell membrane properties, a pharmacological target that has not been explored yet. 

REFERENCES

- Escudero, A., J. C. Montilla, J. M. Garcia, M. C. Sanchez-Quevedo, J. L. Periago, P. Hortelano, and M. D. Suarez. 1998. Effect of dietary (n-9), (n-6) and (n-3) fatty acids on membrane lipid composition and morphology of rat erythrocytes. *Biochim. Biophys. Acta*. **1394**: 65–73.
- Vicario, I. M., D. Malkova, E. K. Lund, and I. T. Johnson. 1998. Olive oil supplementation in healthy adults: effects in cell membrane fatty acid composition and platelet function. *Ann. Nutr. Metab.* **42**: 160–169.
- Zicha, J., J. Kunes, and M. A. Devynck. 1999. Abnormalities of membrane function and lipid metabolism in hypertension: a review. *Am. J. Hypertens.* **12**: 315–331.
- Escriba, P. V., J. M. Sanchez-Dominguez, R. Alemany, J. S. Perona, and V. Ruiz-Gutierrez. 2003. Alteration of lipids, G proteins, and PKC in cell membranes of elderly hypertensives. *Hypertension*. **41**: 176–182.
- Barceló, F., J. S. Perona, J. Prades, S. S. Funari, E. Gomez-Garcia, M. Conde, R. Estruch, and V. Ruiz-Gutierrez. 2009. Mediterranean-style diet effect on the structural properties of erythrocyte cell membrane of hypertensive patients: the Prevencion con Dieta Mediterranea Study. *Hypertension*. **54**: 1143–1150.
- Kinnunen, P. K. J. 1996. On the molecular-level mechanisms of peripheral protein-membrane interactions induced by lipids forming inverted non-lamellar phases. *Chem. Phys. Lipids*. **81**: 151–166.
- Lee, A. G. 2004. How lipids affect the activities of integral membrane proteins. *Biochim. Biophys. Acta*. **1666**: 62–87.
- Escriba, P. V. 2006. Membrane-lipid therapy: a new approach in molecular medicine. *Trends Mol. Med.* **12**: 34–43.
- Lewis, A. H., D. A. Mannock, and R. N. McElhaney. 1997. Membrane lipid molecular structure and polymorphism. In *Lipid Polymorphism and Membrane Properties*. R. Epand, editor. Academic Press, San Diego. 25–102.
- Siegel, D. P., and R. M. Epand. 1997. The mechanism of lamellar-to-inverted hexagonal phase transitions in phosphatidylethanolamine: implications for membrane fusion mechanisms. *Biophys. J.* **73**: 3089–3111.
- Botelho, A. V., N. J. Gibson, R. L. Thurmond, Y. Wang, and M. F. Brown. 2002. Conformational energetics of rhodopsin modulated by nonlamellar-forming lipids. *Biochemistry*. **41**: 6354–6368.
- Vogler, O., J. Casas, D. Capo, T. Nagy, G. Borchert, G. Martorell, and P. V. Escriba. 2004. The Gbetagamma dimer drives the interaction of heterotrimeric Gi proteins with nonlamellar membrane structures. *J. Biol. Chem.* **279**: 36540–36545.
- Funari, S. S., F. Barcelo, and P. V. Escriba. 2003. Effects of oleic acid and its congeners, elaidic and stearic acids, on the structural properties of phosphatidylethanolamine membranes. *J. Lipid Res.* **44**: 567–575.
- Prades, J., S. S. Funari, P. V. Escriba, and F. Barcelo. 2003. Effects of unsaturated fatty acids and triacylglycerols on phosphatidylethanolamine membrane structure. *J. Lipid Res.* **44**: 1720–1727.
- Barcelo, F., J. Prades, S. S. Funari, J. Frau, R. Alemany, and P. V. Escriba. 2004. The hypotensive drug 2-hydroxyoleic acid modifies the structural properties of model membranes. *Mol. Membr. Biol.* **21**: 261–268.
- Prades, J., R. Alemany, J. S. Perona, S. S. Funari, O. Vogler, V. Ruiz-Gutierrez, P. V. Escriba, and F. Barcelo. 2008. Effects of 2-hydroxyoleic acid on the structural properties of biological and model plasma membranes. *Mol. Membr. Biol.* **25**: 46–57.
- Alemany, R., S. Teres, C. Baamonde, M. Benet, O. Vogler, and P. V. Escriba. 2004. 2-hydroxyoleic acid: a new hypotensive molecule. *Hypertension*. **43**: 249–254.
- Alemany, R., O. Vogler, S. Teres, C. Egea, C. Baamonde, F. Barcelo, C. Delgado, K. H. Jakobs, and P. V. Escriba. 2006. Antihypertensive action of 2-hydroxyoleic acid in SHR via modulation of the protein kinase A pathway and Rho kinase. *J. Lipid Res.* **47**: 1762–1770.
- Mozaffarian, D., M. B. Katan, A. Ascherio, M. J. Stampfer, and W. C. Willett. 2006. Trans fatty acids and cardiovascular disease. *N. Engl. J. Med.* **354**: 1601–1613.
- Constantinou-Kokotou, V., V. Magrioti, and R. Verger. 2004. Sterically hindered triacylglycerol analogues as potent inhibitors of human digestive lipases. *Chemistry*. **10**: 1133–1140.
- Lindahl, E., B. Hess, and D. van der Spoel. 2001. GROMACS 3.0: a package for molecular simulation and trajectory analysis. *J. Mol. Model.* **7**: 306–317.
- Cordomi, A., O. Edholm, and J. J. Perez. 2008. Effect of ions on a dipalmitoyl phosphatidylcholine bilayer: a molecular dynamics simulation study. *J. Phys. Chem. B*. **112**: 1397–1408.
- Knecht, V., A. E. Mark, and S. J. Marrink. 2006. Phase behavior of a phospholipid/fatty acid/water mixture studied in atomic detail. *J. Am. Chem. Soc.* **128**: 2030–2034.
- Wong-Ekkabut, J., Z. Xu, W. Triampo, I. M. Tang, D. P. Tieleman, and L. Monticelli. 2007. Effect of lipid peroxidation on the properties of lipid bilayers: a molecular dynamics study. *Biophys. J.* **93**: 4225–4236.
- Leekumjorn, S., H. J. Cho, Y. Wu, N. T. Wright, A. K. Sum, and C. Chan. 2009. The role of fatty acid unsaturation in minimizing biophysical changes on the structure and local effects of bilayer membranes. *Biochim. Biophys. Acta*. **1788**: 1508–1516.
- Cordomi, A., O. Edholm, and J. J. Perez. 2007. Effect of different treatments of long-range interactions and sampling conditions in molecular dynamic simulations of rhodopsin embedded in a dipalmitoyl phosphatidylcholine bilayer. *J. Comput. Chem.* **28**: 1017–1030.
- Cordomi, A., and J. J. Perez. 2007. Molecular dynamics simulations of rhodopsin in different one-component lipid bilayers. *J. Phys. Chem. B*. **111**: 7052–7063.
- Berger, O., O. Edholm, and F. Jähnig. 1997. Molecular dynamics simulations of a fluid bilayer of dipalmitoylphosphatidylcholine at full hydration, constant pressure, and constant temperature. *Biophys. J.* **72**: 2002–2013.
- Petrache, H. I., S. W. Dodd, and M. F. Brown. 2000. Area per lipid and acyl length distributions in fluid phosphatidylcholines determined by H-2 NMR spectroscopy. *Biophys. J.* **79**: 3172–3192.
- Leekumjorn, S., and A. K. Sum. 2006. Molecular simulation study of structural and dynamic properties of mixed DPPC/DPPE bilayers. *Biophys. J.* **90**: 3951–3965.
- Leekumjorn, S., and A. K. Sum. 2007. Molecular studies of the gel to liquid-crystalline phase transition for fully hydrated DPPC and DPPE bilayers. *Biochim. Biophys. Acta*. **1768**: 354–365.

32. Schuttelkopf, A. W., and D. M. F. van Aalten. 2004. PRODRG: a tool for high-throughput crystallography of protein-ligand complexes. *Acta Crystallogr. D Biol. Crystallogr.* **60**: 1355–1363.
33. Small, D. M., D. J. Cabral, D. P. Cistola, J. S. Parks, and J. A. Hamilton. 1984. The ionization behavior of fatty acids and bile acids in micelles and membranes. *Hepatology*. **4**: 77S–79S.
34. Hamilton, J. A. 1998. Fatty acid transport: difficult or easy? *J. Lipid Res.* **39**: 467–481.
35. Hofsäss, C., E. Lindahl, and O. Edholm. 2003. Molecular dynamics simulations of phospholipid bilayers with cholesterol. *Biophys. J.* **84**: 2192–2206.
36. Wohlert, J., and O. Edholm. 2004. The range and shielding of dipole-dipole interactions in phospholipid bilayers. *Biophys. J.* **87**: 2433–2445.
37. Seelig, J., P. M. Macdonald, and P. G. Scherer. 1987. Phospholipid head groups as sensors of electric charge in membranes. *Biochemistry*. **26**: 7535–7541.
38. Vigh, L., I. Horvath, B. Maresca, and J. L. Harwood. 2007. Can the stress protein response be controlled by 'membrane-lipid therapy'? *Trends Biochem. Sci.* **32**: 357–363.
39. Epand, R. M., R. F. Epand, N. Ahmed, and R. Chen. 1991. Promotion of hexagonal phase formation and lipid mixing by fatty acids with varying degrees of unsaturation. *Chem. Phys. Lipids*. **57**: 75–80.
40. Vogler, O., A. Lopez-Bellan, R. Alemany, S. Tofe, M. Gonzalez, J. Quevedo, V. Pereg, F. Barcelo, and P. V. Escriba. 2008. Structure-effect relation of C18 long-chain fatty acids in the reduction of body weight in rats. *Int. J. Obes.* **32**: 464–473.